Stem Cell Reports

Report

Atypical PKC and Notch Inhibition Differentially Modulate Cortical Interneuron Subclass Fate from Embryonic Stem Cells

David J. Tischfield,[1,2] Junho Kim,[2] and Stewart A. Anderson[1,2,*]
[1]Neuroscience Graduate Group, Perelman School of Medicine, University of Pennsylvania, Philadelphia, PA 19104-6085, USA
[2]Department of Psychiatry, Children's Hospital of Philadelphia, University of Pennsylvania School of Medicine ARC 517, Philadelphia, PA 19104-5127, USA
*Correspondence: sande@mail.med.upenn.edu
http://dx.doi.org/10.1016/j.stemcr.2017.03.015

SUMMARY

Recent studies indicate that the location of neurogenesis within the medial ganglionic eminence (MGE) critically influences the fate determination of cortical interneuron subgroups, with parvalbumin (Pv) interneurons originating from subventricular zone divisions and somatostatin (Sst) interneurons primarily arising from apical divisions. The aPKC-CBP and Notch signaling pathways regulate the transition from apical to basal progenitor and their differentiation into post-mitotic neurons. We find that aPKC inhibition enhances intermediate neurogenesis from stem cell-derived MGE progenitors, resulting in a markedly increased ratio of Pv- to Sst-expressing interneurons. Conversely, inhibition of Notch signaling enriches for Sst subtypes at the expense of Pv fates. These findings confirm that the mode of neurogenesis influences the fate of MGE-derived interneurons and provide a means of further enrichment for the generation of specific interneuron subgroups from pluripotent stem cells.

INTRODUCTION

Proper function of the cerebral cortex requires the coordinated activity of two distinct neuronal populations: excitatory projection neurons and inhibitory GABAergic interneurons (cINs). In both mice and humans, roughly half of all cINs originate within the medial ganglionic eminence (MGE) of the subcortical telencephalon and can be separated into two non-overlapping categories defined by their expression of either parvalbumin (Pv) or somatostatin (Sst) (Kepecs and Fishell, 2014; Kubota and Kawaguchi, 1994). While Sst interneurons primarily target the dendrites of their synaptic partners, Pv interneurons mainly target the cell body, proximal dendrites, or the axon initial segment of pyramidal neurons (Rudy et al., 2011). Interneuron dysfunction is implicated in major neurological and psychiatric diseases including autism, schizophrenia, and epilepsy (Marin, 2012).

Due to their remarkable capacity to migrate, survive, and integrate into cortical circuitry after transplantation, cINs are attractive candidates for use in cell-based therapies of disorders of cortical inhibition, such as epilepsy (Southwell et al., 2014; Tyson and Anderson, 2014). Although progress has been made in generating enriched populations of interneuron subgroups from pluripotent stem cells (Harmacek et al., 2014; Tyson et al., 2015), protocols to efficiently generate highly enriched samples of Pv interneurons are lacking.

We recently demonstrated that Pv interneurons originate primarily from divisions of intermediate progenitors in the subventricular zone (SVZ) of the MGE (Petros et al., 2015). This finding is consistent with a previous study that loss of cyclin D2 (Ccnd2), which is expressed in inter-

mediate progenitors throughout the telencephalon, results in reduced numbers of Pv interneurons without affecting the Sst-expressing subgroup (Glickstein et al., 2007). Loss of Nr2f1, which results in increased expression of Ccnd2 in the dorsal region of the MGE where most Sst interneurons normally originate (Inan et al., 2012), also results in supernumerary production of Pv interneurons (Lodato et al., 2011). Together, these findings suggest that enhancement of intermediate progenitor-like divisions should enhance the production of Pv interneurons from stem cell differentiation.

The atypical protein kinase C (aPKC)-CREB-binding protein (CBP) signaling pathway regulates the differentiation of interneurons from ventral forebrain neural progenitors (Tsui et al., 2014). Activation of aPKC results in the phosphorylation of CREB, thereby promoting neural differentiation (Wang et al., 2010). In addition, aPKC is an integral component of the aPKC/Par complex that regulates cell polarity and the localization of cell-fate determinants (Vorhagen and Niessen, 2014) including the Notch inhibitor Numb (Klezovitch et al., 2004). Since aPKC inhibition enhances intermediate neurogenesis in the neocortex (Wang et al., 2012), we examined whether aPKC inhibition during directed differentiations of embryonic stem cells (ESCs) into cortical interneurons will bias progenitors to undergo SVZ-like divisions. We find that a PKC pseudo-substrate peptide inhibitor (aPKCi), applied to our "MGE" protocol (Tyson et al., 2015), significantly increases the fraction of these progenitors that express Ccnd2. Moreover, treatment of stem cell differentiations with aPKCi greatly enriches for the generation of Pv-expressing interneurons at the expense of those expressing Sst. Also consistent with our studies in vivo (Petros et al., 2015), Notch

signaling inhibition promotes the generation of Sst subtype fate. Taken together, our system provides a platform for further study of cortical interneuron genesis, fate determination, and their use in the development of cell-based therapies.

RESULTS

Generation of Nkx2.1-Expressing Interneuron Progenitors

Our previous study used a dual-reporter mouse ESC (mESC) line for the isolation of interneuron-fated cells at the progenitor and post-mitotic stages (Tyson et al., 2015). This line expresses mCherry and GFP under the control of the Nkx2.1 and Lhx6 loci in bacterial artificial chromosomes, respectively. The line can be differentiated using a modified version of our previously established protocol (Figure 1A; Maroof et al., 2010; Tyson et al., 2015) into a highly enriched population of FoxG1- and Nkx2.1-expressing MGE-like progenitors. Although only ∼11% of all Nkx2.1$^+$ cells express mCherry by differentiation day 11 (DD11), nearly all mCherry-expressing cells also express Nkx2.1 protein, confirming the fidelity of the reporter (Figures 1B and 1C). Thus, this system serves as an excellent platform for studying stem cell-derived MGE-like progenitors in vitro.

Atypical PKC Inhibition Increases the Fraction of Cyclin D2-Expressing Nkx2.1::mCherry Progenitors

We reasoned that if inhibition of aPKC biases neocortical progenitors toward intermediate neurogenesis (Wang et al., 2012), treatment of differentiations with the aPKCi beginning at DD8, when most of the cells in the culture express Nkx2.1, should increase the fraction of Nkx2.1::mCherry progenitors that also express Ccnd2. Indeed, aPKCi significantly increased the percentage of Ccnd2-expressing mCherry and Nkx2.1-positive progenitors (Figures 1D and 1E). To determine whether the effect of aPKCi on Ccnd2 expression by Nkx2.1$^+$ progenitors is more broadly applicable to other stem cell lines and clones, we differentiated several additional mESC lines using the same protocol and found that aPKCi significantly increased the fraction of Nkx2.1-expressing progenitors that also express Ccnd2 (Figure S1).

To determine whether aPKCi treatment also influences progenitor proliferation, we pulsed cells for 30 min with the S-phase marker 5-ethynyl-2′-deoxyuridine (EdU), together with immunostaining for the proliferation marker Ki-67. Analysis of both markers showed no significant change in the fraction of EdU or Ki-67 expressing mCherry and Nkx2.1-positive progenitors with aPKCi treatment (Figure S2). These results suggest that aPKCi biases progenitors

toward intermediate neurogenesis without affecting overall proliferation.

Atypical PKC Inhibition Influences the Mode of Neurogenesis

The expression of mCherry and GFP in our mESC line enables us to evaluate whether the outcome of a division is proliferative or neurogenic. Using time-lapse confocal microscopy, we found that from DD8 to DD10 an Nkx2.1::mCherry progenitor could divide into two mCherry-positive progenitors that then go on to divide again into Nkx2.1::mCherry$^+$ cells (Figures 2A and 2B; Movie S1). Other examples include symmetrical neurogenic divisions in which a mCherry-expressing progenitor divides to produce two Lhx6::GFP, post-mitotic interneuron precursors, which have visibly enhanced migratory activity (Figures 2C and 2D; Movie S2). On rare occasions, more complex division schemes could be visualized, incorporating both symmetrical proliferative, symmetrical neurogenic, and asymmetrical neurogenic divisions (Figures 2E and 2F; Movie S3).

Using this system, we hypothesized that aPKCi treatment should increase the fraction of Nkx2.1::mCherry daughter cells that divide symmetrically to produce two progenitors. Indeed, we found that aPKCi nearly doubled the percentage of Nkx2.1::mCherry progenitors that were observed to undergo a second division. Together with the increased co-labeling of Nkx2.1-expressing progenitors with Ccnd2, these results suggest that aPKCi biases interneuron progenitors to undergo SVZ-like divisions (Figure 2G).

Atypical PKC Inhibition Enhances Pv Fate Specification

Since directing MGE progenitors to undergo SVZ divisions directs them to produce Pv-expressing cortical interneurons in vivo (Petros et al., 2015), and since the aPKCi enhances the generation of SVZ-like progenitors in vitro, we next asked whether this treatment enhances the derivation of Pv interneurons relative to Sst interneurons in our stem cell system. mCherry$^+$ progenitors differentiated in the presence or absence of aPKCi were isolated at day 11 via fluorescence-activated cell sorting (FACS) and transplanted into neonatal mouse neocortex (Figure 3A). Following transplantation, the mCherry reporter downregulates as the Lhx6::GFP reporter becomes expressed in the post-mitotic interneuron precursors and is maintained in those cells thereafter (Figure 3B; Tyson et al., 2015). Thirty days post transplantation, the fates of transplanted cells was assayed via immunostaining for GFP, Pv, and Sst. aPKCi-treated cultures resulted in a tremendous enrichment of Pv-expressing interneurons at the expense of those expressing Sst (Figures 3C and 3D). Immunostaining for the MGE-derived cIN marker Sox6, together with GABA,
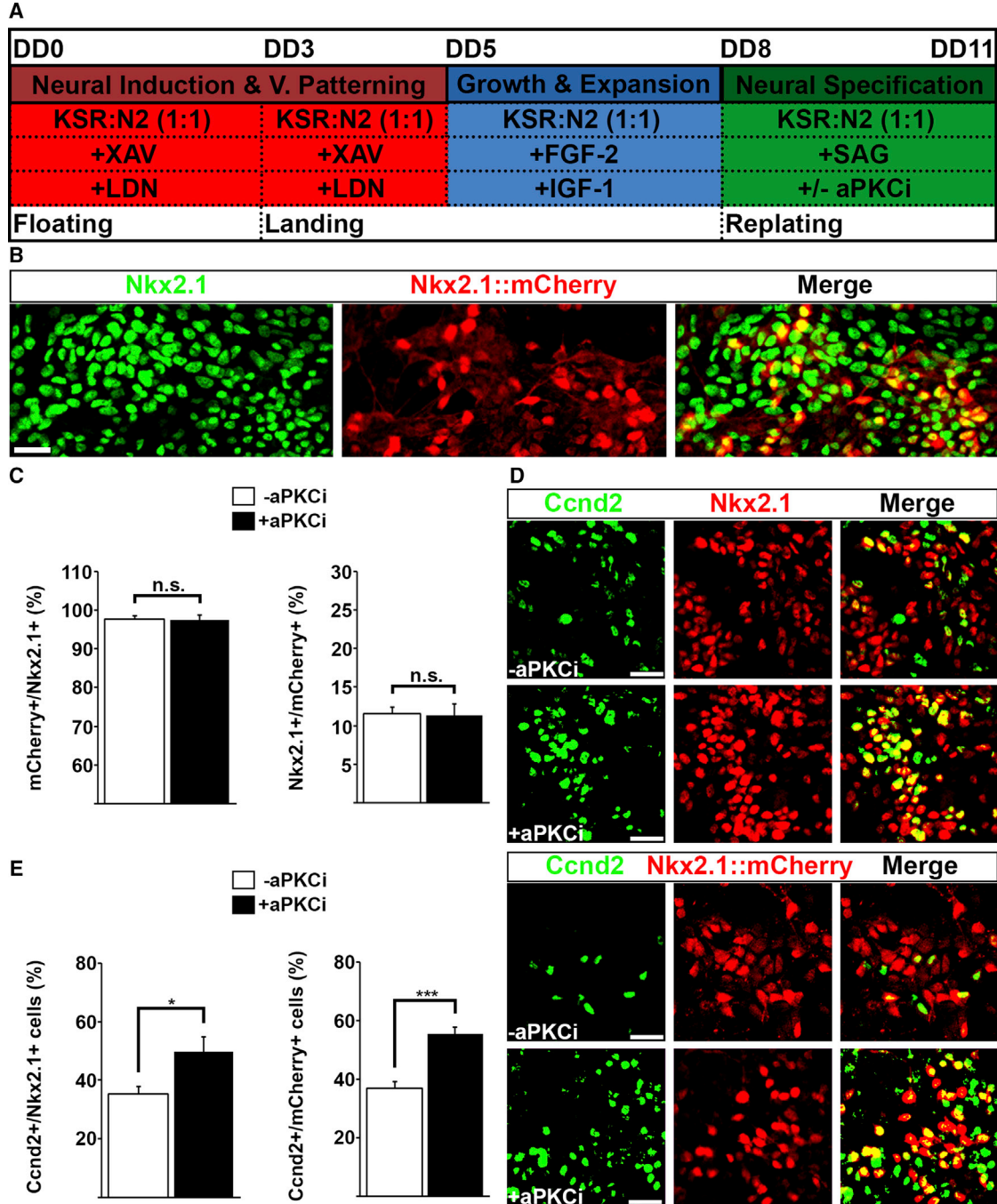
Figure 1. aPKCi Increases the Proportion of Ccnd2-Expressing Nkx2.1 MGE Progenitors

(A) Schematic of the differentiation protocol, with and without the addition of aPKCi from differentiation day 8 (DD8) to DD11.

(B) Representative immunostaining of Nkx2.1 and Nkx2.1::mCherry from the JQ27 line at DD11 differentiated via the protocol shown in (A).

(C) Quantification of the percentage of Nkx2.1::mCherry cells that also express Nkx2.1 protein, as well as the percentage of Nkx2.1^{+} cells that express Nkx2.1::mCherry. Neither of these measures is affected by aPKCi treatment.

(D) Ccnd2 with Nkx2.1::mCherry and Nkx2.1 immunofluorescence on DD11 cultures grown with and without aPKCi from DD8 to DD11.

(E) Quantification of the percentage of Nkx2.1 and Nkx2.1::mCherry-expressing cells that express Ccnd2 shows a significant increase in the aPKCi treated condition.

Error bars indicate SEM. *p < 0.05; ***p < 0.001; n.s., not significant (pooled data from four independent experiments). All scale bars represent 30 μm.
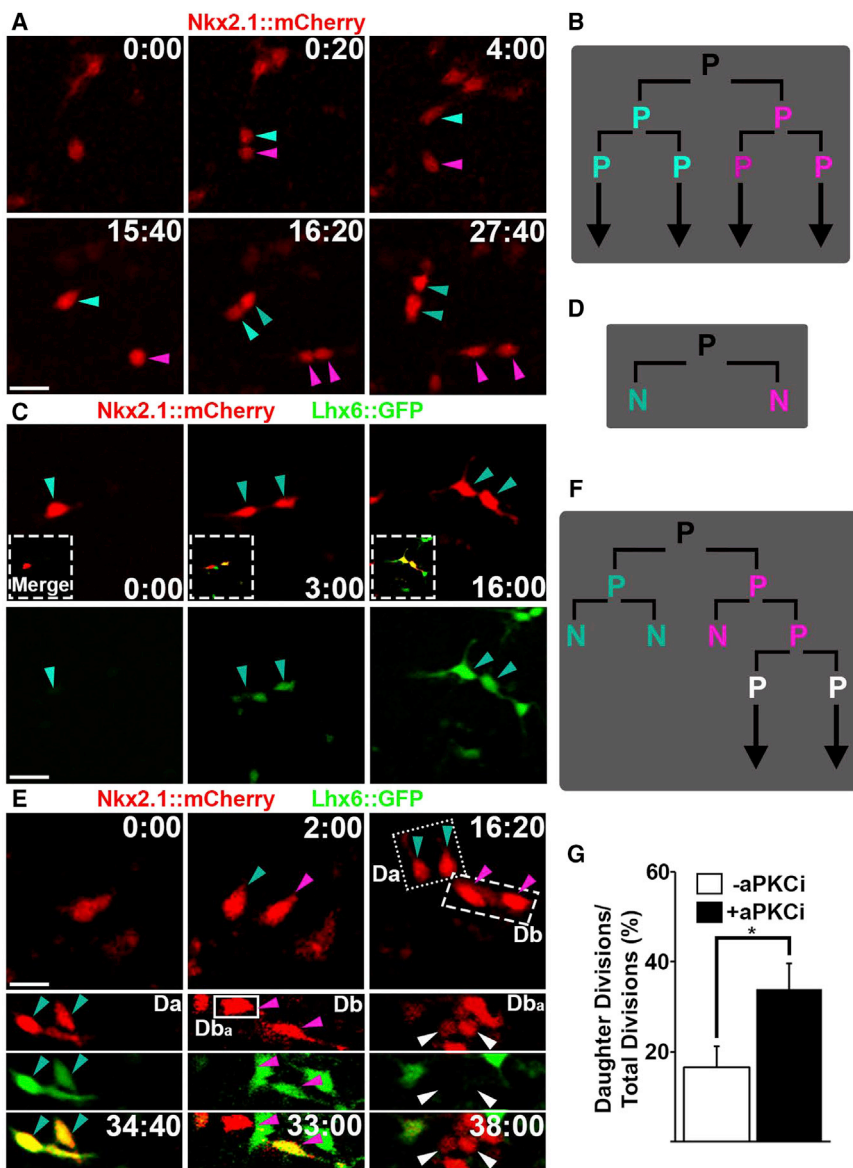
Figure 2. Live Cell Imaging Enables Analysis of Cell Divisions and Shows that aPKCi Increases the Proportion of Nkx2.1::mCherry Daughter Cells that Undergo a Second Division

(A) A series of time-lapse images showing a single Nkx2.1::mCherry progenitor dividing symmetrically to produce two mCherry-expressing progenitors, which then go on to divide again during the 48-hr imaging session. Time is displayed as (hours:minutes).

(B) Lineage relationships between cells in (A).

(C) A series of time-lapse images showing a symmetrical neurogenic division, wherein one Nkx2.1::mCherry progenitor divides symmetrically to produce two Lhx6::GFP daughter cells. Merge of GFP and mCherry channels is shown in dashed inset.

(D) Lineage relationships between cells in (C).

(E) Time-lapse imaging showing a more complex division scheme involving symmetrical proliferative, symmetrical neurogenic, and asymmetrical neurogenic divisions.

(F) Lineage relationships between cells in (E).

(G) Quantification of the number of daughter cell divisions, defined by a Nkx2.1::mCherry daughter from a previous division that goes on to divide again. The number of daughter divisions is divided by the total number of Nkx2.1::mCherry divisions counted. The addition of aPKCi significantly increases the percentage of Nkx2.1::mCherry progenitors that divide again (pooled data from five independent experiments; 95 divisions counted in −aPKCi-treated condition, 84 divisions counted in +aPKCi-treated condition; $*p < 0.05$). Error bars indicate SEM. All scale bars represent 30 μm.

confirms that aPKCi-treated cells retain the appropriate lineage markers (Figure S3).

Notch Inhibition Promotes Cell-Cycle Exit and Enhances Sst Fate Specification

Since aPKCi treatment enhances SVZ-like neurogenesis and Pv fate, we reasoned that early cell-cycle exit would reduce the capacity for progenitors to undergo intermediate neurogenesis and limit the generation of Pv subtypes. We recently used a similar strategy utilizing in utero electroporation of a dominant-negative version of the Mastermind-like-1 protein (dnMAML) to inhibit Notch signaling and drive apical progenitors out of the cell cycle (Petros et al.,

2015). This resulted in a dramatic increase in the fraction of Sst subtypes produced at the expense of Pv fates in vivo (Petros et al., 2015). To determine whether Notch inhibition has the same effect of promoting Sst fate in our stem cell system, we applied the γ-secretase inhibitor DAPT ((S)-tert-butyl 2-((S)-2-(2-(3,5-difluorophenyl)acetamido) propanamido)-2-phenylacetate), which inhibits Notch signaling by blocking cleavage of the Notch intracellular domain (Dovey et al., 2001; Geling et al., 2002), to our stem cell cultures from DD12 to DD14 (Figure 4A). Using the Lhx6::GFP reporter expression as a measure of cell-cycle exit, we found that application of DAPT (10 μM) causes a ~2-fold increase in the fraction of Lhx6::GFP+ and
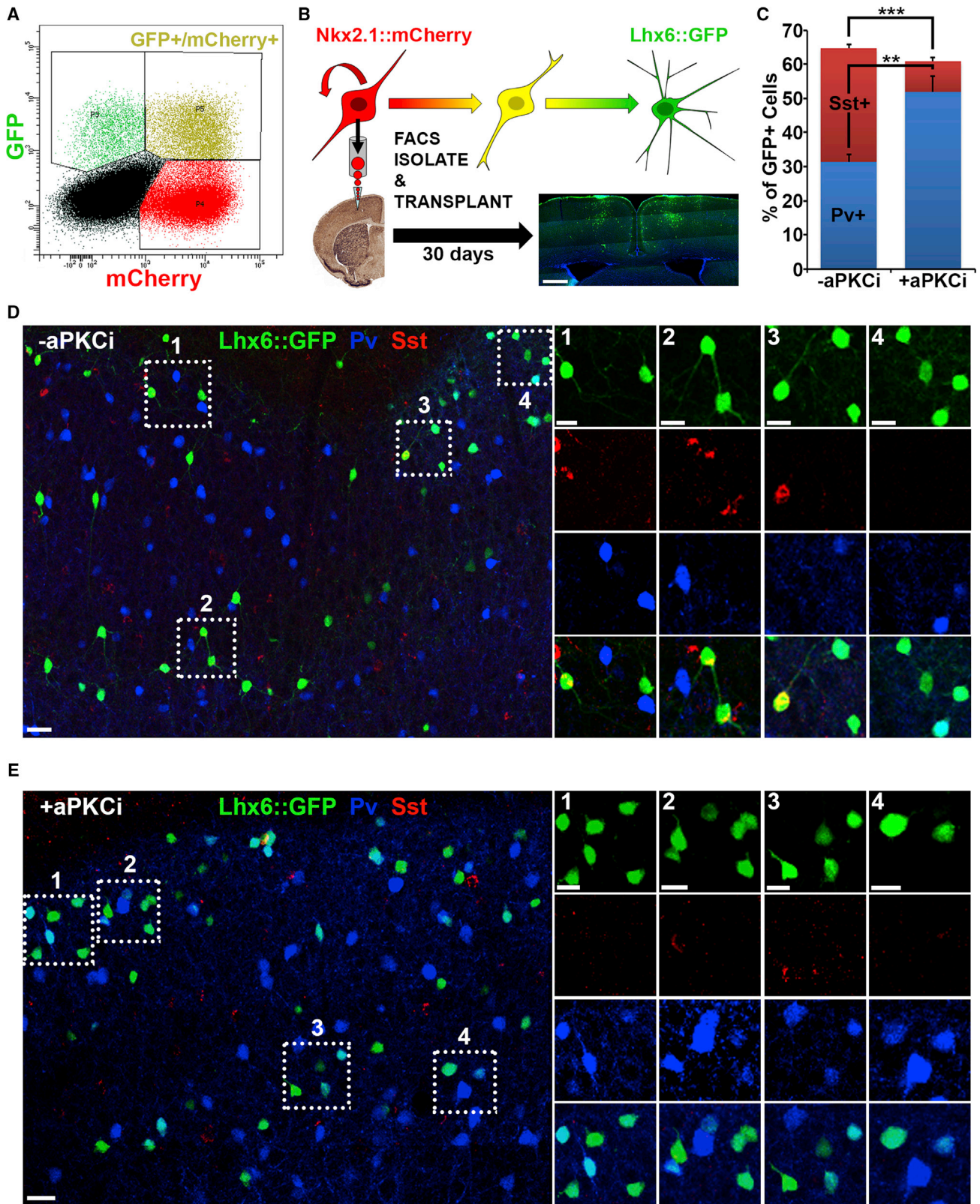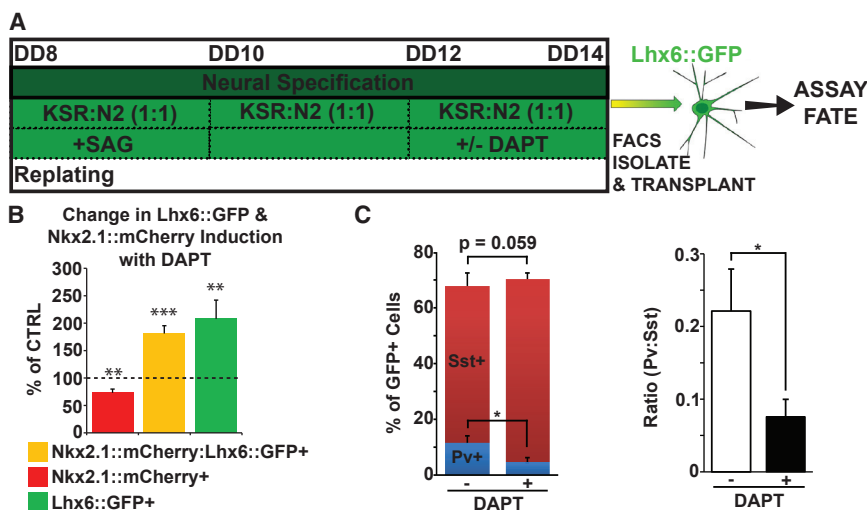
(legend on next page)

Figure 4. Notch Inhibition Induces Cell-Cycle Exit and Biases Progenitors toward Sst Fates

(A) Schematic of the differentiation protocol, with and without the addition of DAPT, from DD12 to DD14. The steps from DD0 to DD8 were identical to those shown in Figure 1A. For these experiments, Lhx6::GFP-only expressing cells grown in the presence or absence of DAPT were collected on DD14 and transplanted into neonatal neocortex for fate analysis.

(B) FACS analysis of the three different populations (Nkx2.1::mCherry, Nkx2.1::mCherry:Lhx6::GFP, and Lhx6::GFP) shows that DAPT causes a 208% ± 34% (**$p < 0.01$) increase in the percentage of Lhx6::GFP-only expressing cells, a 181% ± 14% (***$p < 0.001$) increase in the percentage of Nkx2.1::mCherry:Lhx6::GFP-double expressing cells, and a 27% ± 7% (**$p < 0.01$) decrease in the percentage of Nkx2.1::mCherry-only expressing cells (error expressed as SEM; n = 5 independent differentiations).

(C) Comparison of the absolute percentage of Pv and Sst cells obtained in the presence and absence of DAPT shows a significant decrease in the percentage of Pv-expressing cells (11.6% ± 2.7% −DAPT versus 4.8% ± 1.4% +DAPT; $p < 0.05$) and a borderline significant increase in the percentage of Sst-expressing cells (56.4.6% ± 4.8% −DAPT versus 65.7% ± 2.3% +DAPT; $p = 0.059$). There was no change in the fraction of double-negative cells (32% ± 3.8% −DAPT versus 29.5% ± 1.3% +DAPT; $p = 0.27$). Comparison of the ratio of Pv to Sst cells obtained in the presence and absence of DAPT showed that there was a significant decrease in the Pv-to-Sst ratio (0.22 ± 0.06 −DAPT versus 0.08 ± 0.02 +DAPT; *$p < 0.05$). Error expressed as SEM, n = 5 independent experiments; 323 cells counted in −DAPT condition, 555 cells counted in +DAPT condition.

Lhx6::GFP:Nkx2.1::mCherry^{+} cells, and a concomitant 27% decrease in the fraction of mCherry-only expressing cells (Figure 4B). These results are consistent with a dramatic shift from cycling MGE-like interneuron progenitors (Nkx2.1[+]) to post-mitotic interneuron precursors (Lhx6^{+}). Next, we isolated Lhx6::GFP^{+} cells on DD14 via FACS and transplanted them into neonatal mouse neocortex for fate analysis (Figure 4A). Although Lhx6::GFP^{+} cells are already strongly biased to become Sst subtypes (Tyson et al., 2015), we found that DAPT application further enhanced the generation of Sst subtypes at the expense of those expressing Pv (Figure 4C).

DISCUSSION

Cortical interneurons occur in heterogeneous populations based on their morphology, connectivity, electrophysiology,

---

Figure 3. Strategy to Enhance the Generation of Parvalbumin-Expressing Interneurons from a Dual Nkx2.1:mCherry-Lhx6:GFP Mouse Stem Cell Reporter Line

(A) Representative FACS plot of the JQ27 line (Tyson et al., 2015) at DD11 shows segregation of mCherry-only (red), mCherry/GFP co-expressing (yellow), and GFP-only (green) expressing populations from non-fluorescent cells (black).

(B) Schematic of reporter progression in mESCs differentiated toward Nkx2.1-and Lhx6-expressing fates, then subjected to FACS for mCherry on DD11, followed by transplantation into neonatal mouse cortex. After 30 days the animals are euthanized and the fates of transplanted cells are assayed.

(C) Quantification of somatostatin (Sst) or parvalbumin (Pv) expression in Lhx6::GFP-expressing cells differentiated in the presence or absence of aPKCi from DD8 to DD11 (−aPKCi: 31.3% ± 2.4% Pv, 33.5% ± 2.14% Sst, and 35.3% ± 0.87% double-negative; +aPKCi: 51.9% ± 4.5% Pv, 9.03% ± 1.4% Sst, and 39.1% ± 3.6% double-negative; ±SEM). The addition of aPKCi from DD8 to DD11 significantly increases the ratio of Pv to Sst cells generated (n = 4 independent differentiations, n = 8 brains total, 1,883 cells were counted in −aPKCi condition, 1,092 cells were counted in +aPKCi condition; **$p < 0.01$, ***$p < 0.001$).

(D) Representative brain section containing transplanted Lhx6::GFP cells from the non-aPKCi-treated condition immunostained for GFP, Pv, and Sst, with high-magnification images of individual cells expressing GFP, Pv, and Sst on the right.

(E) Representative brain section containing transplanted Lhx6::GFP cells from the aPKCi treated condition immunostained for GFP, Pv, and Sst, with high-magnification images of individual cells expressing GFP, Pv, and Sst on the right.

Scale bars represent 20 μm (D and E), 400 μm (B), and 10 μm (high-magnification insets).

and neurochemical profiles. As a consequence, interneuron subtypes differentially influence cortical functions. Accordingly, dysfunction of distinct interneuron subtypes is implicated in the pathobiology of major neurological and psychiatric diseases. Thus, considerable effort is being put forth to generate specific interneuron subgroups or subtypes from ESCs. The capacity to do so would not only allow for the study of factors that regulate the type, number, or function of interneurons, but would also enable their use in cell-based therapies.

Our previous study showed that manipulations of sonic hedgehog (Shh) exposure and time in culture differentially enrich for Pv- versus Sst-fated mESC-derived cINs (Tyson et al., 2015). While early-born cells exposed to higher levels of Shh produced a ~6.4:1 ratio of Sst to Pv, increased duration in culture combined with lower levels of Shh generated a ~2.6:1 ratio of Pv to Sst. Another study using the forced expression of transcription factors in a gain-of-function approach found that Lmo3 expression after the expression of Nkx2.1 and Dlx2 was able to achieve a 2.7:1 ratio of Pv to Sst (Harmacek et al., 2014). In this study, we used aPKC inhibition to achieve a ~5.8:1 ratio of Pv to Sst. This, to our knowledge, is the best enrichment for Pv-expressing subtypes that has been obtained from mESCs to date.

Although it remains unclear how aPKCi promotes intermediate neurogenesis in the context of our "MGE" differentiation system, there are several intriguing possibilities. First, the aPKC subgroup contains two isoforms, *iota* (ι or λ) and *zeta* (ζ), which have been shown to have numerous, distinct functions in the regulation of cell polarity, proliferation, and neural differentiation (Fatt et al., 2015; Vorhagen and Niessen, 2014; Wang et al., 2012). Loss of aPKCλ in mouse stem cells enhances self-renewal through the activation of Notch1 and its downstream effectors (Mah et al., 2015). Similarly, in dorsal neocortex, knockdown of aPKCλ delays neural differentiation and expands the pool of Tbr2+ intermediate progenitors, whereas knockdown of aPKCζ promotes radial glia self-renewal (Wang et al., 2012). These studies show that aPKCλ and aPKCζ promote stem cell differentiation through partially overlapping pathways. In our system we use transient, partial inhibition of both aPKC isoforms to enhance the production of Ccnd2+ intermediate progenitors. We favor the idea that partial inhibition of both isoforms promotes a balance between differentiation and self-renewal, resulting in the expansion of basal progenitors. This idea is supported by studies in *Drosophila melanogaster*, which show that aPKC is required to restrict the localization of cell-fate determinants into the differentiating daughter cell via its interactions with the par complex. Inhibition of aPKC disrupts the par complex and promotes daughter cell self-renewal (Goulas et al., 2012). Additional studies focusing on the selective loss of either isoform during interneuron genesis are needed to determine their individual roles. Such knowledge might have profound implications for generating interneuron subtypes from stem cells.

In the field of cancer biology, aPKCs have generated considerable interest due to their roles in driving cellular proliferation. Interestingly, in basal cell carcinomas, aPKCλ forms a complex with missing-in metastasis (MIM) that potentiates Shh signaling (Atwood et al., 2013). Genetic or pharmacological loss of aPKCλ blocks Shh signaling and cancer cell proliferation. Previous in vitro and in vivo studies from our laboratory have shown that lower levels of Shh signaling preferentially bias MGE progenitors to Pv-expressing interneuron fates (Tyson et al., 2015; Xu et al., 2010). It is tempting to speculate that aPKCi may also bias progenitors to produce Pv-fated interneurons through manipulation of Shh signaling. In fact, loss of Shh signaling in embryonic mice initially reduces proliferation in the MGE ventricular zone while simultaneously upregulating it in the MGE SVZ (Xu et al., 2005). Taken together, our study provides evidence that aPKCs play a role in cortical interneuron fate determination and may be doing so through interactions with the Notch and Shh signaling pathways.

EXPERIMENTAL PROCEDURES

mESC Culture

mESCs (the JQ27 mESC-Nkx2.1::mCherry:Lhx6::GFP line) were grown on mouse embryonic fibroblasts (MEF CF-1 MITC7M, GSC-6101M, Global Stem) in standard mESC medium (knockout DMEM [Invitrogen], 15% fetal bovine serum [Invitrogen-Thermo Fisher Scientific] supplemented with L-glutamine, minimum essential medium non-essential amino acids, β-mercaptoethanol, and leukemia inhibitory factor [1.4 μL/mL [10^7 U/mL] ESG1107, Millipore]). mESCs were replated on a 0.1% gelatin-coated plate for 1–2 days prior to differentiation to eliminate MEFs.

Telencephalic mESC Differentiation

For neural induction, mESCs were harvested and floated on non-tissue culture treated plates in a 1:1 mixture of KSR (10828-028, Invitrogen) and N2 medium (DMEM/F12, Invitrogen catalog #11330, with N2, Stemgent #07156) supplemented with LDN-193189 (250 nM, Stemgent #04-0074) and XAV939 (10 μM, Stemgent #04-0046) as described previously (Maroof et al., 2010; Watanabe et al., 2005). At DD3, embryoid bodies (EBs) were enzymatically dissociated using Accutase (Invitrogen #A1110501) and single cells were replated onto poly-L-Lysine-coated (Sigma #P6282) and laminin-coated (Sigma #L2020) plates (37,500 cells/cm^2) in the same medium supplemented with Y-27632 (10 nM, Tocris #1254). For the dorsal/ventral (D/V) patterning, cells were treated with KSR/N2 medium supplemented with fibroblast growth factor 2 (10 ng/mL, DD5–9, R&D Systems #233-FB), IGF1 (20 ng/mL, days 5–9, R&D Systems

291-G1-200/CF) from DD5 to DD8. At DD8, cells were replated on PLL- and LN-coated plates at 200,000 cells/cm^2 and treated with KSR/N2 medium supplemented with smoothened agonist (SAG) (30 nM, EMD Biosciences) and protein kinase C ζ Inhibitor (PKCi) (2 μM, EMD Biosciences). Cells were cultured until DD11 and then processed for FACS or IHC. For experiments involving the use of DAPT (10 μM, Sigma #D5942), cells were replated on DD8 with SAG from DD8 to DD10. On DD10, the medium was changed without any additional growth factors. On DD12, DAPT was added and remained in the medium until processing on DD14.

In Vivo Fate Quantification

Care of animals was in accordance with institutional guidelines at The Children's Hospital of Philadelphia. Thirty days post transplantation, mice were perfused and fixed with 4% paraformaldehyde in PBS. Fixed brains were sectioned in the coronal plane at 50 μm on a vibrating microtome (Leica). For identification of the fate of the transplanted cells, sections including somatosensory cortex, rostral to the hippocampal commissure and caudal to the genu of the corpus collosum, were incubated with the aforementioned antibodies. Generally 12–15 sections were evaluated per marker. Transplanted animals were excluded if there were fewer than 25 total GFP$^+$ cells present, and only GFP$^+$ cells engrafted in cortical layers 2–6 were included in fate analysis. Each condition was repeated on four separate occasions, with a minimum of two transplanted mice per condition. Therefore, a statistical n represents counts from multiple transplants of one differentiation experiment. Statistical significance was determined using a two-tailed Student's t test.

SUPPLEMENTAL INFORMATION

Supplemental Information includes Supplemental Experimental Procedures, three figures, and three movies and can be found with this article online at http://dx.doi.org/10.1016/j.stemcr.2017.03.015.

AUTHOR CONTRIBUTIONS

D.J.T. and J.K. performed the experiments. D.J.T., J.K., and S.A.A. designed experiments and wrote the manuscript.

ACKNOWLEDGMENTS

REFERENCES

Atwood, S.X., Li, M., Lee, A., Tang, J.Y., and Oro, A.E. (2013). GLI activation by atypical protein kinase C iota/lambda regulates the growth of basal cell carcinomas. Nature 494, 484–488.

Dovey, H.F., John, V., Anderson, J.P., Chen, L.Z., de Saint Andrieu, P., Fang, L.Y., Freedman, S.B., Folmer, B., Goldbach, E., Holsztynska, E.J., et al. (2001). Functional gamma-secretase inhibitors reduce beta-amyloid peptide levels in brain. J. Neurochem. 76, 173–181.

Fatt, M., Hsu, K., He, L., Wondisford, F., Miller, F.D., Kaplan, D.R., and Wang, J. (2015). Metformin acts on two different molecular pathways to enhance adult neural precursor proliferation/self-renewal and differentiation. Stem Cell Rep. 5, 988–995.

Geling, A., Steiner, H., Willem, M., Bally-Cuif, L., and Haass, C. (2002). A gamma-secretase inhibitor blocks Notch signaling in vivo and causes a severe neurogenic phenotype in zebrafish. EMBO Rep. 3, 688–694.

Glickstein, S.B., Moore, H., Slowinska, B., Racchumi, J., Suh, M., Chuhma, N., and Ross, M.E. (2007). Selective cortical interneuron and GABA deficits in cyclin D2-null mice. Development 134, 4083–4093.

Goulas, S., Conder, R., and Knoblich, J.A. (2012). The Par complex and integrins direct asymmetric cell division in adult intestinal stem cells. Cell Stem Cell 11, 529–540.

Harmacek, L., Watkins-Chow, D.E., Chen, J., Jones, K.L., Pavan, W.J., Michael Salbaum, J., and Niswander, L. (2014). A unique missense allele of BAF155, a core BAF chromatin remodeling complex protein, causes neural tube closure defects in mice. Dev. Neurobiol. 74, 483–497.

Inan, M., Welagen, J., and Anderson, S.A. (2012). Spatial and temporal bias in the mitotic origins of somatostatin- and parvalbumin-expressing interneuron subgroups and the chandelier subtype in the medial ganglionic eminence. Cereb. Cortex 22, 820–827.

Kepecs, A., and Fishell, G. (2014). Interneuron cell types are fit to function. Nature 505, 318–326.

Klezovitch, O., Fernandez, T.E., Tapscott, S.J., and Vasioukhin, V. (2004). Loss of cell polarity causes severe brain dysplasia in Lgl1 knockout mice. Genes Dev. 18, 559–571.

Kubota, Y., and Kawaguchi, Y. (1994). Three classes of GABAergic interneurons in neocortex and neostriatum. Jpn. J. Physiol. 44, S145–S148.

Lodato, S., Tomassy, G.S., De Leonibus, E., Uzcategui, Y.G., Andolfi, G., Armentano, M., Touzot, A., Gaztelu, J.M., Arlotta, P., Menendez de la Prida, L., et al. (2011). Loss of COUP-TFI alters the balance between caudal ganglionic eminence- and medial ganglionic eminence-derived cortical interneurons and results in resistance to epilepsy. J. Neurosci. 31, 4650–4662.

Mah, I.K., Soloff, R., Hedrick, S.M., and Mariani, F.V. (2015). Atypical PKC-iota controls stem cell expansion via regulation of the notch pathway. Stem Cell Rep. 5, 866–880.

Marin, O. (2012). Interneuron dysfunction in psychiatric disorders. Nat. Rev. Neurosci. 13, 107–120.

Maroof, A.M., Brown, K., Shi, S.H., Studer, L., and Anderson, S.A. (2010). Prospective isolation of cortical interneuron precursors from mouse embryonic stem cells. J. Neurosci. 30, 4667–4675.

Petros, T.J., Bultje, R.S., Ross, M.E., Fishell, G., and Anderson, S.A. (2015). Apical vs. basal neurogenesis directs cortical interneuron subclass fate. Cell Rep. 13, 1090–1095.

Rudy, B., Fishell, G., Lee, S., and Hjerling-Leffler, J. (2011). Three groups of interneurons account for nearly 100% of neocortical GABAergic neurons. Dev. Neurobiol. *71*, 45–61.

Southwell, D.G., Nicholas, C.R., Basbaum, A.I., Stryker, M.P., Kriegstein, A.R., Rubenstein, J.L., and Alvarez-Buylla, A. (2014). Interneurons from embryonic development to cell-based therapy. Science *344*, 1240622.

Tsui, D., Voronova, A., Gallagher, D., Kaplan, D.R., Miller, F.D., and Wang, J. (2014). CBP regulates the differentiation of interneurons from ventral forebrain neural precursors during murine development. Dev. Biol. *385*, 230–241.

Tyson, J.A., and Anderson, S.A. (2014). GABAergic interneuron transplants to study development and treat disease. Trends Neurosci. *37*, 169–177.

Tyson, J.A., Goldberg, E.M., Maroof, A.M., Petros, T.P., and Anderson, S.A. (2015). Duration of culture and Sonic Hedgehog signaling differentially specify PV versus SST cortical interneuron fates from embryonic stem cells. Development *142*, 1267–1278.

Vorhagen, S., and Niessen, C.M. (2014). Mammalian aPKC/Par polarity complex mediated regulation of epithelial division orientation and cell fate. Exp. Cell Res. *328*, 296–302.

Wang, J., Weaver, I.C., Gauthier-Fisher, A., Wang, H., He, L., Yeomans, J., Wondisford, F., Kaplan, D.R., and Miller, F.D. (2010). CBP histone acetyltransferase activity regulates embryonic neural differentiation in the normal and Rubinstein-Taybi syndrome brain. Dev. Cell *18*, 114–125.

Wang, J., Gallagher, D., DeVito, L.M., Cancino, G.I., Tsui, D., He, L., Keller, G.M., Frankland, P.W., Kaplan, D.R., and Miller, F.D. (2012). Metformin activates an atypical PKC-CBP pathway to promote neurogenesis and enhance spatial memory formation. Cell Stem Cell *11*, 23–35.

Watanabe, K., Kamiya, D., Nishiyama, A., Katayama, T., Nozaki, S., Kawasaki, H., Watanabe, Y., Mizuseki, K., and Sasai, Y. (2005). Directed differentiation of telencephalic precursors from embryonic stem cells. Nat. Neurosci. *8*, 288–296.

Xu, Q., Wonders, C.P., and Anderson, S.A. (2005). Sonic hedgehog maintains the identity of cortical interneuron progenitors in the ventral telencephalon. Development *132*, 4987–4998.

Xu, Q., Guo, L., Moore, H., Waclaw, R.R., Campbell, K., and Anderson, S.A. (2010). Sonic hedgehog signaling confers ventral telencephalic progenitors with distinct cortical interneuron fates. Neuron *65*, 328–340.